Journal of Photochemistry & Photobiology, B: Biology 217 (2021) 112145

Contents lists available at ScienceDirect

Journal of Photochemistry & Photobiology, B: Biology

journal homepage: www.elsevier.com/locate/jphotobiol

Photosynthesis and calcification of the coccolithophore *Emiliania huxleyi* are more sensitive to changed levels of light and CO_2 under nutrient limitation

Yong Zhang [a,b], Kunshan Gao [a,c,*]

[a] State Key Laboratory of Marine Environmental Science, College of Ocean and Earth Sciences, Xiamen University, Xiamen, China
[b] College of Environmental Science and Engineering, Fujian Key Laboratory of Pollution Control and Resource Recycling, Fujian Normal University, Fuzhou, China
[c] Co-Innovation Center of Jiangsu Marine Bio-industry Technology, Jiangsu Ocean University, Lianyungang 222005, China

ARTICLE INFO

Keywords:
Calcification
Coccolithophore
CO_2
Light
Nutrient limitation
Photosynthesis

ABSTRACT

Photophysiological responses of phytoplankton to changing multiple environmental drivers are essential in understanding and predicting ecological consequences of ocean climate changes. In this study, we investigated the combined effects of two CO_2 levels (410 and 925 μatm) and five light intensities (80 to 480 μmol photons m^{-2} s^{-1}) on cellular pigments contents, photosynthesis and calcification of the coccolithophore *Emiliania huxleyi* grown under nutrient replete and limited conditions, respectively. Our results showed that high light intensity, high CO_2 level and nitrate limitation acted synergistically to reduce cellular chlorophyll *a* and carotenoid contents. Nitrate limitation predominantly enhanced calcification rate; phosphate limitation predominantly reduced photosynthetic carbon fixation rate, with larger extent of the reduction under higher levels of CO_2 and light. Reduced availability of both nitrate and phosphate under the elevated CO_2 concentration decreased saturating light levels for the cells to achieve the maximal relative electron transport rate ($rETR_{max}$). Light-saturating levels for $rETR_{max}$ were lower than that for photosynthetic and calcification rates under the nutrient limitation. Regardless of the culture conditions, *rETR* under growth light levels correlated linearly and positively with measured photosynthetic and calcification rates. Our findings imply that *E. huxleyi* cells acclimated to macronutrient limitation and elevated CO_2 concentration decreased their light requirement to achieve the maximal electron transport, photosynthetic and calcification rates, indicating a photophysiological strategy to cope with CO_2 rise/pH drop in shoaled upper mixing layer above the thermocline where the microalgal cells are exposed to increased levels of light and decreased levels of nutrients.

1. Introduction

Increasing emissions of anthropogenic CO_2 are responsible for ocean acidification (OA) and ocean warming [1], which enhances water column stratification, thus shoaling the upper mixed layer (UML), increasing daily integrative exposures of solar radiation to the cells within the layer and reducing upward transport of nutrients into it [2]. As a consequence, phytoplankton cells dwelling in the UML are experiencing concurrent changes in multiple drivers that affect primary production and carbon cycles in the surface ocean [3–5].

Coccolithophores take up CO_2 and produce both particulate organic carbon (POC) through photosynthesis and particulate inorganic carbon (PIC, $CaCO_3$) via calcification [6–8]. Within ocean ecosystems, coccolithophores contribute about 20% to total organic carbon fixation [9] and up to 50% of $CaCO_3$ flux to marine sediments [10,11]. Therefore, this important phytoplankton group plays an important role in marine biological carbon and carbonate pumps [6]. Consequently, their responses to climate changes are gaining increasing attentions [12–14]. Calcification of coccolithophores and other marine calcifiers is known to susceptible to OA. It has been documented that the cosmopolitan and bloom-forming coccolithophore *Emiliania huxleyi* reduces calcification rate and increases photosynthetic rate under OA, reducing PIC to POC ratios [12,13]. Nevertheless, responses of coccolithophores to OA are modulated by light levels [15,16], nutrients availability [17,18], temperature [19], UV radiation [4,16] and species-, population- and strain-specific traits [20–22], and are dependent on different carbonate

* Corresponding author at: State Key Laboratory of Marine Environmental Science, College of Ocean and Earth Sciences, Xiamen University, Xiamen, China.
E-mail address: ksgao@xmu.edu.cn (K. Gao).

https://doi.org/10.1016/j.jphotobiol.2021.112145
Received 29 October 2020; Received in revised form 2 January 2021; Accepted 25 January 2021
Available online 2 February 2021
1011-1344/© 2021 Elsevier B.V. All rights reserved.

chemistry backgrounds [23] and regional adaptation [24].

Light absorbed by photosynthetic organisms provides energy for assimilation processes and energy transfer in adenosine triphosphate (ATP) and reduced nicotinamide adenine dinucleotide phosphate (NADPH), which are used to take up nutrients, fix CO_2 and produce $CaCO_3$ in coccolithophores [6,25]. It is known that light intensity [15,26,27], light/dark cycle (light period) [28,29] and light quality (including UV radiation) [30–33] alter responses of photosynthesis and calcification of *E. huxleyi* to elevated CO_2 concentrations and associated drop of pH. High light intensities or a continuous (without dark period) light exposure may cancel out the positive effects of rising CO_2 on photosynthetic rates [15,29], and high levels of solar radiation also appear to conteract the negative effect of OA on calcification rate [32]. Presence of UV radiation exacerbates the negative effect of OA on calcification rate [33]. However, most of these studies have tested for interactive roles of light with different CO_2 levels under nutrient replete conditions [26–33]. Only a few studies have reported that increasing light intensity enhanced [34] or did not change [35] the positive impact of rising CO_2 on photosynthetic rates of *E. huxleyi* under nutrient limitation. Little has documented on calcification and photochemical responses of *E. huxleyi* to concurrent changes in light intensity, CO_2 level and nutrients availability [35,36].

Emiliania huxleyi blooms usually occur after the disappearance of diatoms when nitrate, phosphate and silicate are limiting [37]. This ecological advantage stems from an extremely high affinity for inorganic phosphorus [38], and an increased expression of alkaline phosphatase which cleaves orthophosphate from various external organic sources under phosphate limitation [39]. Furthermore, *E. huxleyi* has high ability to take up ammonium, urea and several amino acids, and assimilate organic nitrogen to support cell division [39]. Due to the tight stoichiometric coupling of carbon (C), nitrogen (N) and phosphorus (P) metabolisms, biochemical responses of *E. huxleyi* to nutrient limitation may synergistically [40–42] or antagonisitically [43] alter the impacts of OA on photosynthetic and calcification rates. On the other hand, reduced photosynthetic rates of *E. huxleyi* in response to nutrient limitation were synergistically lowered by decreasing light intensities [34,35]. Only a few studies have assessed responses of cellular PIC content of *E. huxleyi* to combinations of nutrient limitation and light intensity, showing that PIC content increased with reduced nutrients availability and increasing light intensity [35,44]. However, to the best of our knowledge, little has been documented on effects of multiple drivers on photochemical processes of coccolithophores, especially on interactions of nutrient limitation, CO_2 level and light intensity.

Previously, we showed that elevated CO_2 concentration exacerbated photo-inhibition of growth rate under reduced availability of phosphate [35], and that reduced availability of nitrogen predominantly enhanced PIC production rate [35]. In the present work, subsequently, we hypothesized that the photochemical performances under nutrient limitation may be responsible for the observed responses of growth rates to ocean acidification even under different levels of light.

2. Materials and Methods

2.1. Experimental Design

Emiliania huxleyi strain PML B92/11 was originally isolated from Norwegian coastal water and obtained from Plymouth Marine Laboratory, United Kingdom. Cells were grown in dilute batch culture with Aquil medium under a 12: 12 h light: dark cycle (light period: 8:00 a.m. to 8:00 p.m.) at 20 °C in a thermo-controlling incubator (GXZ, Dongnan Instrument Company). The Aquil medium was prepared according to Sunda et al. [45] with the addition of 2200 μM bicarbonate, resulting in initial total alkalinity (TA) of 2200 μM. Initial dissolved inorganic nitrogen (DIN) and phosphorus (DIP) concentrations in Aquil were 100 μM and 10 μM, respectively (HNHP, phase I, Fig. S1). For Aquil medium with low DIN and high DIP concentration (LNHP, phase II), and high DIN and low DIP concentration (HNLP, phase III), the nitrate and phosphate concentrations were set to 8 μM and 10 μM, 100 μM and 0.4 μM, respectively (Table 1).

To examine the combined effects of two levels of CO_2 and five levels of light on *E. huxleyi* grown under different availability of the macronutrients, at each nutrient level, we first established 2 "baseline" CO_2 treatments where ambient CO_2 (LC) and elevated CO_2 (HC) levels were employed. There were 4 replicate flasks for each of LC and HC treatments, with a total of 8 flasks at the beginning of the experiment. To achieve the target CO_2 levels in culture medium, seawater was aerated for 24 h with filtered (PVDF 0.22 μm pore size, Simplepure, Haining) air of 400 μatm (LC, pumped from outside of the building) or 1000 (HC) μatm pCO_2, which was obtained with a CO_2 enriching device (CE100B, Wuhan Ruihua Instrument & Equipment Ltd., China). The dry air/CO_2 mixture was humidified with deionized water before aeration to minimize evaporation. The LC and HC seawaters were, respectively, filtered (0.22 μm pore size, Polycap 75 AS, Whatman) and carefully pumped into sterilized (autoclaved) 500 mL polycarbonate bottles (Nalgene, 4 replicate bottles for each of LC and HC) with no headspace to minimize gas exchange. Then the cells were inoculated to achieve an initial concentration of about 200 cells mL^{-1}. The samples were initially cultured at 80 ± 5 μmol photons $m^{-2} s^{-1}$ of photosynthetically active radiation (PAR) (measured using a PAR Detector, PMA 2132 from Solar Light Company) in LC and HC conditions for 8 generations (5 days) for preculture. Samples in culture bottles were mixed twice a day at 9:00 a.m. and 6:00 p.m. Subsequently, the cultures were diluted to the initial cell concentrations (about 200 cells mL^{-1}) and grown for another 8 generations in the main experiment cultures (5 days). Then sub-samples were taken for measurements of TA, pH_T (total scale), nutrient concentrations, chlorophyll fluorescence parameters, cell concentration, pigments, photosynthetic C-fixation and calcification rates.

After that, the cells (4 bottles for each of LC and HC) of the same initial concentrations as above were transferred stepwise from 80 ± 5 μmol photons $m^{-2} s^{-1}$ to 120 ± 8 μmol photons $m^{-2} s^{-1}$, then to 200 ± 17 μmol photons $m^{-2} s^{-1}$, 320 ± 16 μmol photons $m^{-2} s^{-1}$ and 480 ± 30 μmol photons $m^{-2} s^{-1}$, and incubated for 8 generations (5 days in 120 and 480 μmol photons $m^{-2} s^{-1}$, 4 days in 200 and 320 μmol photons $m^{-2} s^{-1}$) at each light intensity, respectively. Then samples were cultured for another 8 generation under each light level before sub-samples were taken as above for measurements of the parameters (Fig. S1). To check whether the sampled cells were in exponential growth phase under each nutrient treatment, we examined cell concentrations every day at LC and 200 ± 17 μmol photons $m^{-2} s^{-1}$ where cells grew faster than in other conditions [35]. Samples were taken and measured daily at 2:00 p.m. (see below). We found that cell concentrations were in the exponential growth phase between the first and the sixth days of the incubation under the HNHP treatment, and between the first and the fifth days of the incubations under the LNHP and HNLP treatments (Fig. S2).

2.2. Nutrient Concentrations and Carbonate Chemistry Measurements

In the first and the last days of the main experiment cultures, 30 mL samples were filtered (0.22 μm pore size, Haining) to measure the

Table 1
Concentrations of dissolved inorganic nitrogen (DIN) and phosphorus (DIP) at the start and end days of the *Emiliania huxleyi* cultures, which lasted for 4–5 days for different treatments, representing 7–8 generations.

		DIN (μM)	DIP (μM)
HNHP	Start	101.1 ± 1.1	10.5 ± 0.2
	End	92.8 ± 1.6	9.7 ± 0.2
LNHP	Start	8.8 ± 0.1	10.3 ± 0.6
	End	1.0 ± 0.4	8.7 ± 0.8
HNLP	Start	99.6 ± 2.3	0.4 ± 0.1
	End	88.5 ± 1.6	< 0.04

dissolved inorganic nitrogen and phosphorus concentrations using a scanning spectrophotometer (Du 800, Beckman Coulter) according to Hansen and Koroleff [46]. The NO_3^- was measured as NO_2^- via the zinc cadmium reduction method. The phosphomolybdenum blue photometric method was used to determine total phosphorus. Measurements of TA and pH_T (total scale) were carried out as in the previous study [35]. Briefly, by maintaining the cell concentrations within a range of 200 to 95,000 cells mL^{-1} with growth periods of 4–5 days, we were able to achieve the pH values of 8.04–8.14 at the start and 8.11–8.16 at the end days of the incubations under LC, respectively; and to attain the pH values of 7.73–7.71 at the start and 7.81–7.88 at the end days of the incubations under HC, respectively. At the end days of the incubations, the carbonate chemistry parameters in all the cultures were significantly different between the HC and LC treatments [35].

2.3. Cell Concentration Measurements

On the last day of the main experiment cultures, ~25 mL samples were taken at the same time (about 2:00 p. m.) as mentioned above. Cell concentrations were measured using a Z2 Coulter Particle Count and Size Analyzer (Beckman Coulter). The diameter of detected particles was set to be 3 to 7 μm in the instrument, which excludes detached coccoliths [17]. Cell concentration was also measured by microscopy (ZEISS), and variation in measured cell concentration between two methods was less than 8%. Average growth rate (μ) was calculated according to the equation: $\mu = (\ln N_t - \ln N_0) / T$, where N_0 was 200 cells ml^{-1} and N_t the cell concentration at the end day of the incubation, and T was the growth period in days. The cell concentrations at the end days of each incubation condition are shown in Table S1.

2.4. Chlorophyll Fluorescence Measurements

The chlorophyll fluorescence parameters were determined using a pulse amplitude modulated fluorometer (Xe-PAM, Walz, Effeltrich, Germany). 3 mL samples were taken from the incubation bottles and kept in the dark for 15 min at 20 °C and used to measure the relative electron transport rate (*rETR*). The assay light levels (A-PAR) were increased from 0 to 1600 μmol photons $m^{-2} s^{-1}$ with 9 steps and 45 s each (Table S2). The instant minimal (F_t) and maximal fluorescence (F_m') were respectively determined at the end of each A-PAR and saturating light pulse (800 ms, 5000 μmol photons $m^{-2} s^{-1}$). According to Baker [47], the effective photochemical quantum yield (*Yield*) was calculated as: $Yield = (F_m' - F_t) / F_m'$. And *rETR* was calculated according to Ralph and Gademann [48] as: $rETR = Yield \times \text{A-PAR}$. The parameters of the photosynthetic response to irradiance (P-I curve) were analyzed as follows: $rETR = rETR_{max} \times \tanh\ (a \times \text{A-PAR}\ /\ rETR_{max})$ according to Jassby and Platt [49]. The maximal relative electron transport rate ($rETR_{max}$) represents light-saturated *rETR*, and light use efficiency (a) was derived from the slop of each *ETR* vs light curve. Saturating light intensity, I_k, is calculated from the expression $rETR_{max} / a$ and represents the onset of light saturation.

2.5. Pigment Measurements

100 mL samples were filtered onto Whatman GF/F glass fiber filters (25 mm) with low vacuum pressure (< 0.02 MPa) and soaked in 5 mL 90% methanol overnight at 4 °C in the dark. The extracts were centrifuged at 5000 ×*g* for 10 min to remove debris and glass fibers. Absorbance of the supernatant from 400 to 800 nm was measured with a scanning spectrophotometer (Du 800, Beckman Coulter, USA). According to Lichtenthaler and Buschmann [50], the chlorophyll *a* (Chl *a*) concentration was calculated as: Chl *a* ($\mu g\ mL^{-1}$) = $16.82 \times (A_{665} - A_{750}) - 9.28 \times (A_{652} - A_{750})$. The carotenoid concentration was calculated as: Carotenoid ($\mu g\ mL^{-1}$) = $[1000 \times (A_{470} - A_{750}) - 1.91 \times \text{Chl } a] / 225$. Where A is the optical density (OD) of supernatant on 750, 665, 652 and 470 nm of wavelength.

2.6. Measurements of Photosynthetic and Calcification Rates

On the last day of the cultures, at the onset of the light period (8:00 a. m.), sub-samples were taken from each incubation bottle, and dispensed into two 24 mL scintillation vials (20 mL samples). Then, 100 μL of 10 μCi (0.37 MBq) $NaH^{14}CO_3$ (ICN Radiochemicals, Irvine, California, USA) were added into 20 mL samples which were incubated under the culture conditions for 12 h. After that, 8 mL samples (two sampling from each treatment: one for photosynthetic carbon fixation, the other for the total carbon fixation of photosynthesis and calcification) were collected and filtered onto Whatman GF/F glass fiber filters (pre-combusted at 450 °C for 6 h) under low pressure (< 0.03 MPa) and dim light, and then rinsed three times with the Aquil medium and stored in the dark at −20 °C. For determination of photosynthetic carbon fixation, the filtered samples (after being thawed) were fumed with HCl for 12 h to remove unincorporated inorganic ^{14}C, and the filtered samples for total carbon fixation via photosynthesis and calcification were not treated with HCl. All samples were dried in a thermostatic oven at 60 °C for 12 h, and digested in 4 mL scintillation cocktail (Hisafe 3, Perkin-Elmer, Shelton, CT, USA), and the amount of ^{14}C incorporated by the samples was counted with a scintillation counter (Tri-Carb 2800TR, Perkin-Elmer, Shelton, CT, USA). The calcification rate was calculated as the difference between the total carbon fixation and photosynthetic carbon fixation rates as reported previously [35].

2.7. Data Analysis

A three-way analysis of variance (ANOVA) was used to determine the main effects of light intensity, CO_2 level, nitrate or phosphate concentrations, and their interactions on the measured parameters. A Tukey Post hoc test was performed to identify the differences between light intensities, two CO_2 levels, two DIN or two DIP concentrations. Normality of residuals was conducted with a Shapiro-Wilk's test and a Levene test was conducted graphically to test for homogeneity of variances. A generalized least squares (GLS) model was used to stabilize heterogeneity if variance was non-homogeneous. All statistical calculations were performed using *R*.

3. Results

3.1. Nutrient Concentrations

During the incubations, dissolved inorganic nitrogen (DIN) concentrations decreased due to the alga's growth, by 8.2% in HNHP, by 88.6% in LNHP and by 11.1% in HNLP conditions, respectively (Table 1). Dissolved inorganic phosphorus (DIP) concentrations decreased by 7.6% in HNHP, by 15.5% in LNHP and by almost 100% (non-detectable) in HNLP conditions, respectively (Table 1).

3.2. Photosynthetic Pigments

Chlorophyll *a* (Chl *a*) and carotenoid quotas showed the same patterns in response to increasing light intensities (Fig. 1A–J). At both LC and HC, both Chl *a* and carotenoid quotas decreased significantly with increasing light intensities regardless of the nutrient treatment (Tukey post hoc, all $p < 0.01$) (Fig. 1A–C, F–H and Table 2). Under HNHP and 80 μmol photons $m^{-2} s^{-1}$, Chl *a* quota was significantly higher in the HC- than LC-grown cells (Tukey post hoc, $p = 0.01$) (Fig. 1A).

Nutrient limitation modulated light responses of Chl *a* and carotenoid quotas (Fig. 1D,E,I,J). In the LC-grown cells, Chl *a* quotas were not significantly different between LNHP and HNHP conditions at any of the tested light levels (Tukey post hoc, all $p > 0.1$); in the HC-grown cells, however, they were lowered by 5.5–40.4% in LNHP than HNHP conditions (Tukey post hoc, $p < 0.01$ at 80 μmol photons $m^{-2} s^{-1}$; $p > 0.1$ at 120–480 μmol photons $m^{-2} s^{-1}$) (Fig. 1D). At LC, carotenoid quotas were lowered by 3.3–32.5% in LNHP than HNHP conditions; at HC, they

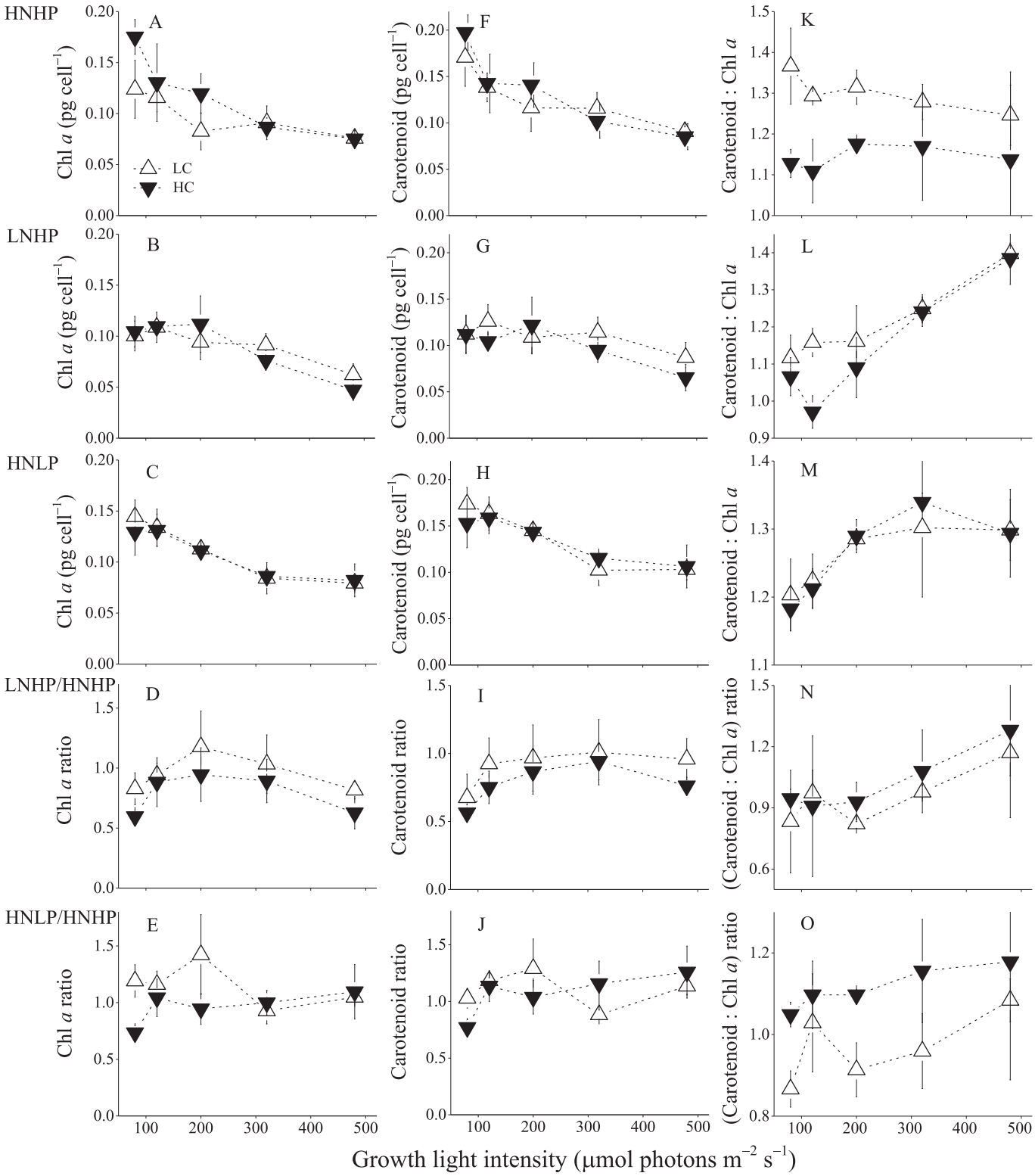

Fig. 1. The chlorophyll *a* (Chl *a*) quota (A–C), carotenoid quota (F-H) and carotenoid to Chl *a* ratio (K–M) as a function of growth light intensity in the *Emiliania huxleyi* cells grown under the high nitrate and high phosphate (HNHP, first row), low nitrate and high phosphate (LNHP, second row), and high nitrate and low phosphate (HNLP, third row) treatments and at ambient pCO_2 (LC, hollow) and elevated pCO_2 levels (HC, solid). The ratios of Chl *a* (D, E), carotenoid (I, J) and (carotenoid: Chl *a*) (N, O) at LNHP to HNHP (fourth row) and at HNLP to HNHP (fifth row), respectively. The data represents the means and standard deviation of four independent cultures.

Table 2
Results of three-way ANOVAs of the effects of dissolved inorganic nitrogen (N) or phosphorus (P) concentrations, pCO_2 levels (C) and light intensities (L) on Chl *a* quota, carotenoid (Car) quota, Car: Chl ratio (Car: Chl), maximal relative electron transport rate ($rETR_{max}$), light use efficiency (*a*), saturated light intensity (I_k), effective photochemical quantum yield (*Yield*), non-photochemical quenching (*NPQ*), photosynthetic carbon fixation rate (Pho), calcification rate (Cal), and calcification: photosynthetic carbon fixation ratio (Cal: Pho) in *E. huxleyi*.

		N	C	L	N × C	N × L	C × L	N × C × L	P	C	L	P × C	P × L	C × L	P × C × L
Chl *a*	F	14.69	3.68	72.76	5.01	7.83	5.19	0.68	142.13	0.07	52.31	1.55	1.28	0.83	3.71
	p	<0.01	=0.06	<0.01	=0.03	<0.01	<0.01	=0.61	<0.01	=0.79	<0.01	=0.22	=0.29	=0.51	<0.01
Car	F	0.77	3.60	44.52	6.83	8.24	2.43	0.23	156.96	0.90	80.02	0.50	2.91	0.16	2.35
	p	=0.38	=0.06	<0.01	=0.01	<0.01	=0.06	=0.92	<0.01	=0.35	<0.01	=0.48	=0.03	=0.96	=0.06
Car: Chl	F	3.47	24.89	20.34	4.256	12.81	2.07	1.81	241.94	0.25	42.47	22.00	8.03	1.13	1.12
	p	=0.07	<0.01	<0.01	=0.04	<0.01	=0.09	−0.14	<0.01	=0.62	<0.01	<0.01	<0.01	=0.35	=0.35
$rETR_{max}$	F	301.50	73.87	442.46	27.21	29.17	40.50	13.76	2.88	2219.07	2070.89	30.08	144.13	40.28	7.14
	p	<0.01	<0.01	<0.01	<0.01	<0.01	<0.01	<0.01	=0.09	<0.01	<0.01	<0.01	<0.01	<0.01	<0.01
a	F	40.25	0.62	2556.33	9.45	4.84	1.62	1.13	2129.60	2032.20	15,928.91	97.82	28.00	15.21	9.70
	p	<0.01	=0.43	<0.01	<0.01	<0.01	=0.18	=0.35	<0.01	<0.01	<0.01	<0.01	<0.01	<0.01	<0.01
I_k	F	521.44	218.10	2318.51	10.19	16.09	10.62	8.3	2019.91	11.87	1951.46	0.22	45.44	17.33	14.35
	p	<0.01	<0.01	<0.01	<0.01	<0.01	<0.01	<0.01	<0.01	<0.01	<0.01	=0.63	<0.01	<0.01	<0.01
Yield	F	10.13	33.61	670.46	11.69	3.41	14.62	12.56	69.33	153.33	999.16	103.87	26.65	7.69	3.56
	p	<0.01	<0.01	<0.01	<0.01	=0.01	<0.01	<0.01	<0.01	<0.01	<0.01	<0.01	<0.01	<0.01	=0.01
NPQ	F	13.64	0.05	3.05	1.80	2.22	0.96	4.75	662.10	32,700.85	56.92	31.74	19.00	0.88	21.24
	p	<0.01	=0.82	=0.06	=0.19	=0.12	=0.39	=0.01	<0.01	<0.01	<0.01	<0.01	<0.01	=0.48	<0.01
Pho	F	73.38	8.71	22.02	1.54	11.57	2.80	3.63	1644.74	170.53	173.38	5.65	26.20	24.20	1.33
	p	<0.01	<0.01	<0.01	=0.22	<0.01	=0.03	=0.01	<0.01	<0.01	<0.01	=0.02	<0.01	<0.01	=0.27
Cal	F	874.57	24.22	187.32	20.27	51.89	6.30	2.23	4.34	0.10	76.01	0.25	12.17	15.75	3.87
	p	<0.01	<0.01	<0.01	<0.01	<0.01	<0.01	=0.08	=0.04	=0.75	<0.01	=0.62	<0.01	<0.01	<0.01
Cal: Pho	F	1574.69	113.78	149.18	64.04	71.61	6.63	0.96	447.66	13.21	23.17	7.78	2.29	7.63	3.57
	p	<0.01	<0.01	<0.01	<0.01	<0.01	<0.01	=0.43	<0.01	<0.01	<0.01	<0.01	=0.07	<0.01	=0.01

were lowered by 5.8–43.7% (Tukey post hoc, under both LC and HC: $p < 0.01$ at 80 μmol photons $m^{-2} s^{-1}$; $p > 0.1$ at 120–480 μmol photons $m^{-2} s^{-1}$) (Fig. 1I). Both Chl *a* and carotenoid quotas did not show significant differences between HNLP and HNHP conditions across all light intensities in both LC- and HC-grown cells (Three-way ANOVA; Tukey post hoc, all $p > 0.1$) (Fig. 1E and J). These results showed that high levels of light and CO_2 synergistically reduced the Chl *a* and carotenoid contents when availability of nitrate was low (Fig. 1D and I), whereas P limitation had insignificant influence on them (Fig. 1E and J).

Under HNHP and HNLP conditions, carotenoids to Chl *a* ratios did not show significant differences among different light levels (Fig. 1K and M). However, under LNHP conditions, they increased significantly at both LC and HC with increasing light intensities (Tukey post hoc, both $p < 0.01$ at LC and HC) (Fig. 1L). The ratios were significantly larger at LC than at HC under the HNHP treatments within the light range of 80–200 μmol photons $m^{-2} s^{-1}$ (Tukey post hoc, all $p < 0.05$) (Fig. 1K). However, under both LNHP and HNLP conditions, they were not significantly different between the LC and HC treatments (Tukey post hoc, all $p > 0.1$) (Fig. 1L and M).

3.3. Photochemical Performances

In all culture conditions, relative electron transport rates (*rETR*) increased with increasing assay light intensities and leveled off after reaching the maximal values (Fig. 2). However, the response patterns of the maximal *rETR* ($rETR_{max}$) to growth light intensities were different between nutrient replete and limited conditions (Fig. 3A–C). Under the HNHP treatments, the LC-grown cells exhibited the highest $rETR_{max}$ at about 320 μmol photons $m^{-2} s^{-1}$, and the HC-grown cells reached the highest $rETR_{max}$ at similar PAR level but declined thereafter by 15.1% at 480 μmol photons $m^{-2} s^{-1}$ ($p < 0.01$) (Figs. 2A–E, 3A and Table 2). In both LNHP and HNLP conditions, $rETR_{max}$ increased significantly at both LC and HC until 200 μmol photons $m^{-2} s^{-1}$, and declined thereafter (all $p < 0.01$) (Figs. 2F–O, 3B and C). At 480 μmol photons $m^{-2} s^{-1}$ of PAR, the elevated level of CO_2 reduced $rETR_{max}$ by 20.0% under HNHP and by 25.2% under HNLP conditions, respectively (Tukey Post hoc, both $p < 0.05$), but did not affect $rETR_{max}$ significantly in LNHP (Fig. 3A–C).

At LC, within the light range of 80–320 μmol photons $m^{-2} s^{-1}$, $rETR_{max}$ values were higher in the LNHP- than HNHP-grown cells (Tukey post hoc, $p = 0.3$ at 80 μmol photons $m^{-2} s^{-1}$; all $p < 0.05$ at 120–320 μmol photons $m^{-2} s^{-1}$), whereas the values were lowered at 480 μmol photons $m^{-2} s^{-1}$ ($p < 0.01$) (Fig. 3D). At HC, $rETR_{max}$ values were higher in LNHP than HNHP, being only significant ($p < 0.01$) at 80 and 200 μmol photons $m^{-2} s^{-1}$ (Fig. 3D). At both LC and HC, $rETR_{max}$ was significantly higher in HNLP than HNHP conditions at 200 μmol photons $m^{-2} s^{-1}$ (both $p < 0.01$) (Fig. 3E). Overall, $rETR_{max}$ was more affected by nitrate limitation and increasing light intensities than by the elevated level of CO_2 and phosphate limitation. Furthermore, nutrient limitation and/or the elevated level of CO_2 reduced saturating light intensity for cells to achieve the highest $rETR_{max}$ (Fig. 3).

At both LC and HC, light use efficiency (*a*) decreased significantly with increasing growth light intensities regardless of the nutrient treatment (all $p < 0.01$) (Fig. 3F–H). Values of *a* did not show significant differences between the HC and LC treatments in HNHP and LNHP conditions (all $p > 0.1$) (Fig. 3F and G), but were significantly lower at HC than at LC in HNLP conditions under 320 and 480 μmol photons $m^{-2} s^{-1}$ (Tukey post hoc, $p = 0.04$ at 320 μmol photons $m^{-2} s^{-1}$; $p < 0.01$ at 480 μmol photons $m^{-2} s^{-1}$) (Fig. 3H and J). The extent of reduction in effective photochemical quantum yield (*Yield*) was greater than the *a*n under nutrient limitation and high CO_2 condition (Fig. 3I,J, S,T).

At both LC and HC, saturating light intensity (I_k) increased significantly with increasing growth light intensities (all $p < 0.01$) (Fig. 3K–M). I_k values were significantly lower at HC than at LC under 480 μmol photons $m^{-2} s^{-1}$ in HNHP condition (Fig. 3K), and were significantly

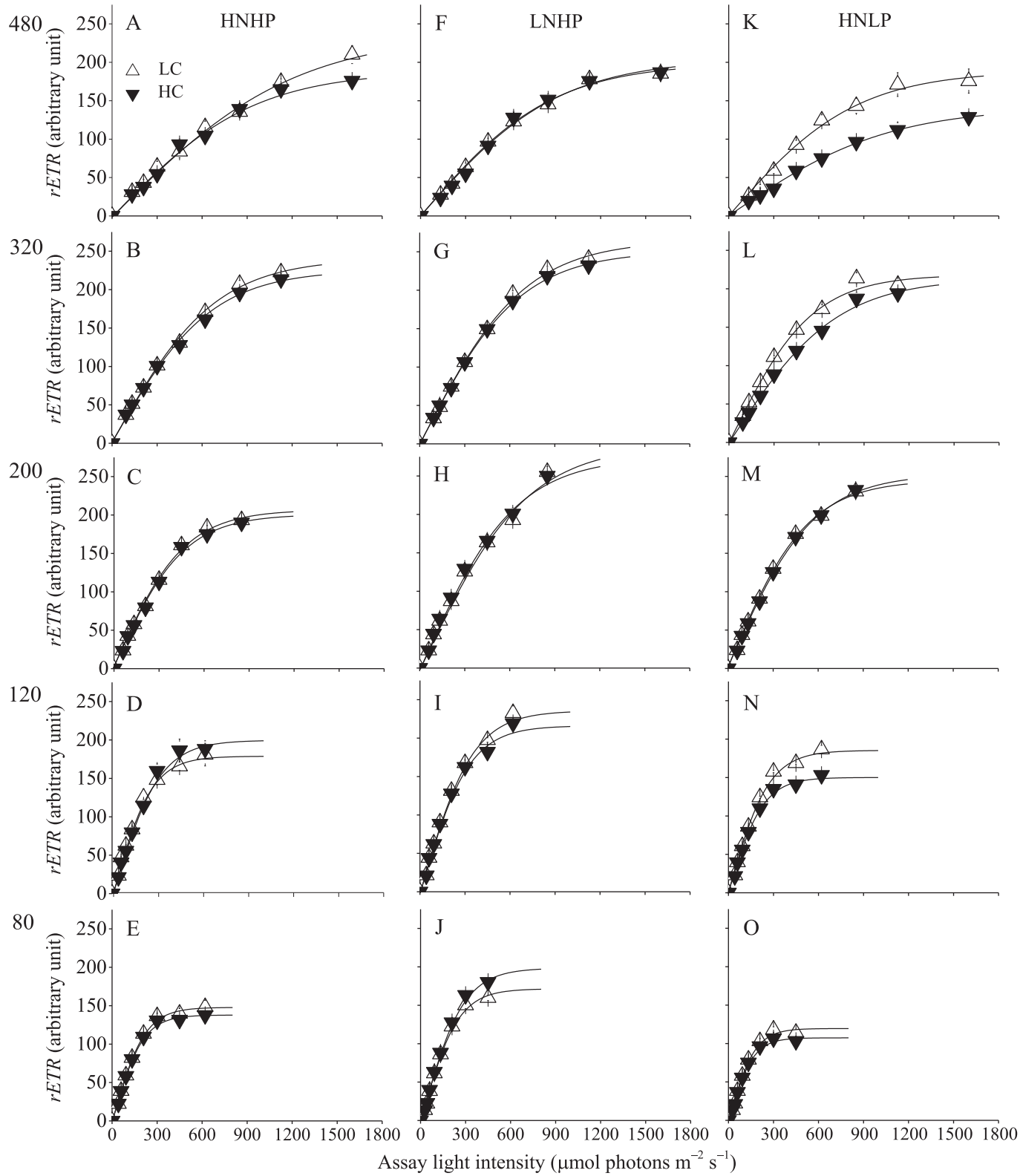

Fig. 2. At each growth light intensity (80, 120, 200, 320 or 480 μmol photons $m^{-2}s^{-1}$), relative electron transport rate (*rETR*) of cells grown at LC (hollow) and HC (solid) under the HNHP (A–E), LNHP (F–J) and HNLP (K-O) treatments as a function of the assay light intensity (0–1600 μmol photons $m^{-2}s^{-1}$), respectively. The lines (*rETR* light–response curves) in each panel were fitted according to Jassby and Platt [49]. The data represents the means and standard deviation of four independent cultures. *rETR* was measured on the fifth culture day at 80, 120 and 480 μmol photons $m^{-2}s^{-1}$, and on the fourth culture day at 200 and 320 μmol photons $m^{-2}s^{-1}$.

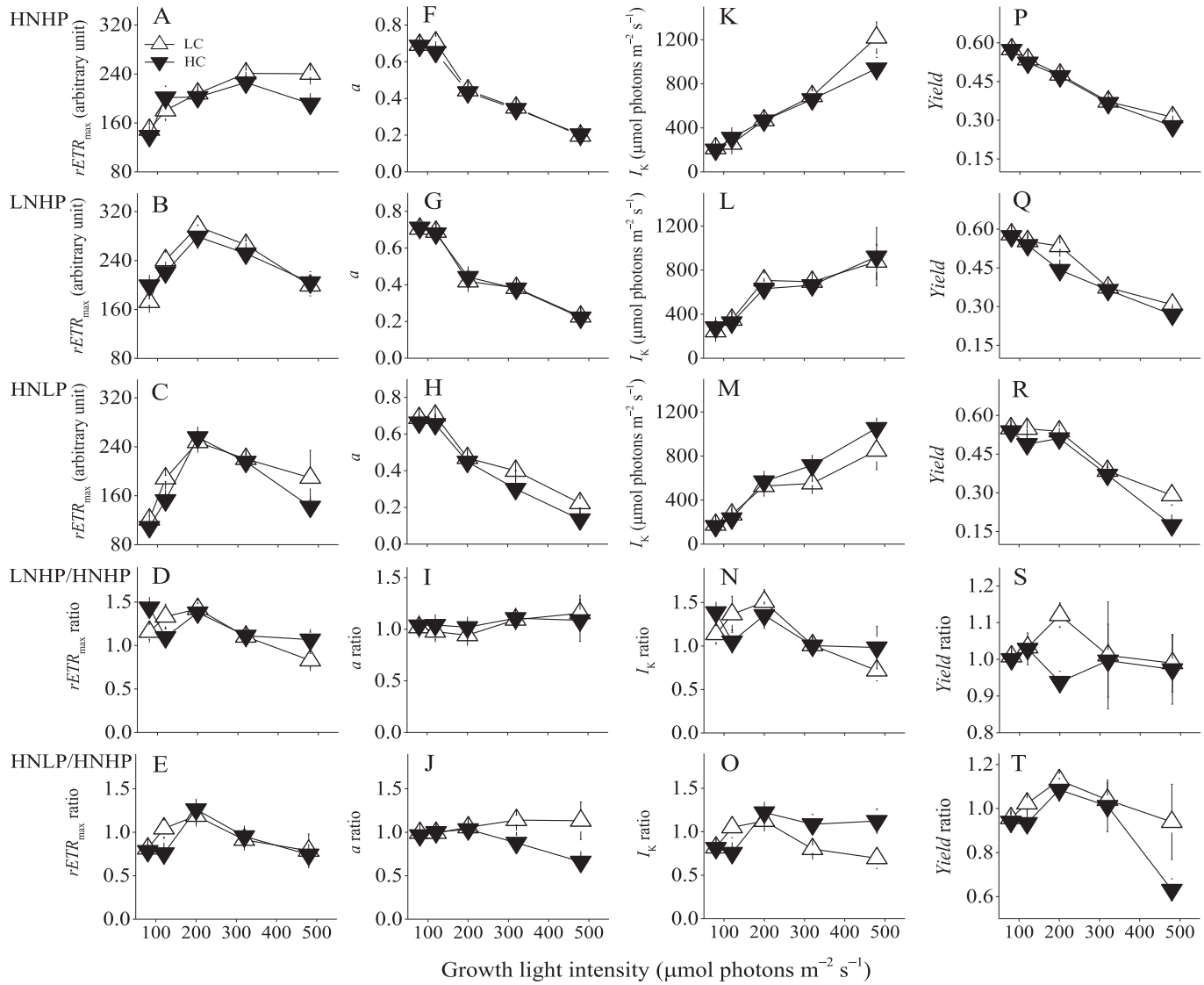

Fig. 3. The maximal relative electron transport rate ($rETR_{max}$) (A–C), light use efficiency (a) (F-H), saturated light intensity (I_k) (K–M) and effective photochemical quantum yield (*Yield*) (P–R) as a function of growth light intensity in the cells grown under the HNHP (first row), LNHP (second row) and HNLP (third row) treatments and at LC (hollow) and HC (solid) levels, respectively. The ratios of $rETR_{max}$ (D, E), a (I, J), I_k (N, O) and *Yield* (S, T) at LNHP to HNHP (fourth row) and at HNLP to HNHP (fifth row), respectively. The data represents the means and standard deviation of four independent cultures. Please see Fig. 2 for detailed information.

larger at HC than at LC under 320 and 480 μmol photons m^{-2} s^{-1} in HNLP conditions (Fig. 3M). At LC, I_k values were significantly higher in LNHP than HNHP conditions under 200 μmol photons m^{-2} s^{-1}; and at HC, they were not significantly different between LNHP and HNHP conditions at each light intensity (Fig. 3N). Under LC and 480 μmol photons m^{-2} s^{-1}, I_k was significantly higher in HNHP than HNLP conditions (Tukey post hoc, $p < 0.01$) (Fig. 3O).

3.4. Photosynthetic Carbon Fixation Rate

Under the HNHP treatments, in the LC- and HC-grown cells, photosynthetic carbon fixation rates (photosynthetic rate) increased significantly with increasing light intensities until 320 μmol photons m^{-2} s^{-1}, and stayed constant thereafter in the former and slightly declined thereafter in the latter ($p = 0.14$) (Fig. 4A). In LNHP conditions, at both LC and HC, they were not significantly different among different light intensities (Tukey Post hoc, df = 4, all $p > 0.1$) (Fig. 4B). In HNLP conditions, they increased significantly with increasing light intensity until 320 μmol photons m^{-2} s^{-1}, and decreased significantly thereafter (both $p < 0.01$ at LC and HC) (Fig. 4C). In HNHP conditions, the light-saturated photosynthetic rates were reduced by 23.9% by the elevated CO_2 treatment ($p < 0.01$) (Fig. 4A); in HNLP conditions, these rates were reduced by 60.8% ($p < 0.01$ at 480 μmol photons m^{-2} s^{-1}) (Fig. 4C).

At both LC and HC, at 320 and 480 μmol photons m^{-2} s^{-1}, photosynthetic rates were reduced by 12.4–32.7% in LNHP than HNHP conditions (at both light intensities: $p < 0.01$ at LC, $p > 0.05$ at HC) (Fig. 4D). At 80–480 μmol photons m^{-2} s^{-1}, photosynthetic rates were significantly lower in HNLP than HNHP conditions at both LC and HC conditions (all $p < 0.01$) (Fig. 4E). Overall, nutrient limitation reduced photosynthetic rates, and in HNLP conditions, these reductions were exacerbated by high levels of light and CO_2 (Fig. 4E). Furthermore, nutrient limitation or elevated level of CO_2 reduced the light intensity for photosynthesis to reach the highest values (Fig. 4A–C).

3.5. Calcification Rate and Calcification: Photosynthesis Ratio

In HNHP conditions, in the LC-grown cells, calcification rates increased significantly with increasing light intensities until 480 μmol

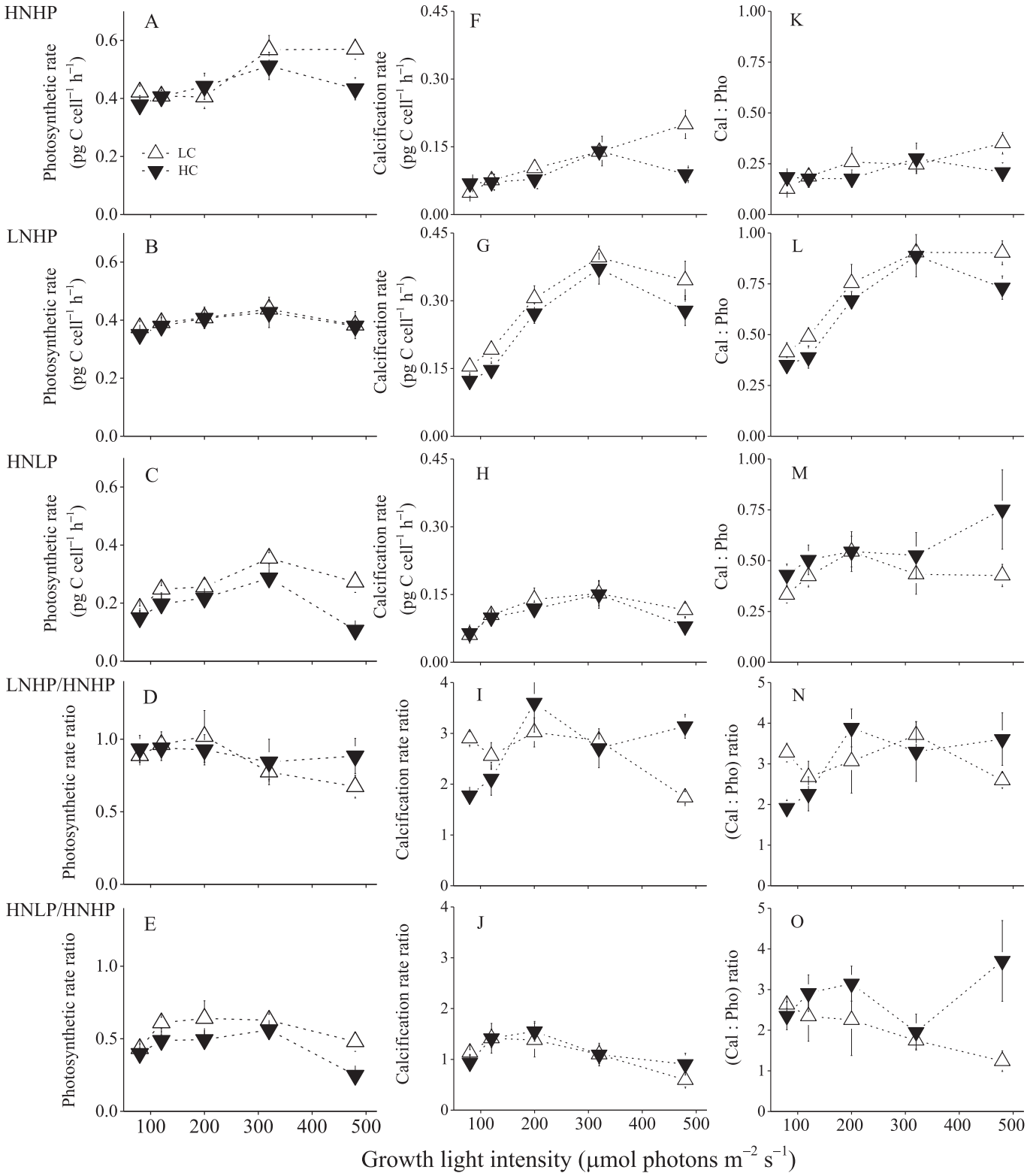

Fig. 4. The photosynthetic rates (A–C), calcification rates (F-H) and calcification to photosynthetic rate ratio (Cal: Pho) (K–M) as a function of growth light intensity in the cells grown under the HNHP (first row), LNHP (second row) and HNLP (third row) treatments and at LC (hollow) and HC (solid) levels, respectively. The ratios of photosynthetic rate (D, E), calcification rate (I, J) and (Cal: Pho) (N, O) at LNHP to HNHP (fourth row) and at HNLP to HNHP (fifth row), respectively. The data represents the means and standard deviation of four independent cultures.

photons $m^{-2} s^{-1}$; in the HC-grown cells, they increased until 320 μmol photons $m^{-2} s^{-1}$ and slightly declined thereafter ($p = 0.20$) (Fig. 4F). In both LNHP and HNLP conditions, calcification rates increased significantly at both LC and HC until 320 μmol photons $m^{-2} s^{-1}$, and declined thereafter (LN: $p = 0.22$ at LC, $p < 0.01$ at HC; LP: $p = 0.44$ at LC, $p < 0.01$ at HC) (Fig. 4G and H). At 480 μmol photons $m^{-2} s^{-1}$, the elevated CO_2 reduced calcification rate under all nutrient treatments ($p < 0.01$ in HNHP; $p = 0.02$ in LNHP; $p = 0.48$ in HNLP) (Fig. 4F–H).

Nitrate limitation enhanced calcification rates. Regardless of light intensities and CO_2 levels, calcification rates were increased by 73.0–248.6% in LNHP compared to HNHP conditions (all $p < 0.01$) (Fig. 4I). Under LC and 480 μmol photons $m^{-2} s^{-1}$, calcification rate was significantly lower at HNLP than HNHP conditions ($p < 0.01$) (Fig. 4J). Overall, the highest calcification rates were observed at a lower growth light intensity for nutrient limited and high CO_2 treatments compared to the nutrient replete and low CO_2 treatments (Fig. 4F–H).

In HNHP conditions, at both LC and HC, calcification: photosynthetic carbon fixation ratios (C: P ratio) increased with increasing light intensities ($p < 0.01$ at LC; $p > 0.1$ at HC) (Fig. 4K). In LNHP conditions, they increased significantly at both LC and HC until 320 μmol photons $m^{-2} s^{-1}$, and leveled off at LC and slightly declined at HC thereafter (both $p > 0.1$) (Fig. 4L). In HNLP conditions, at LC, they increased by 64.1% until 200 μmol photons $m^{-2} s^{-1}$ and slightly declined thereafter ($p = 0.78$); at HC, they increased by 74.7% until 480 μmol photons $m^{-2} s^{-1}$ ($p < 0.01$) (Fig. 4M). Regardless of light intensities and CO_2 levels, C: P ratios were 90.8–278.6% larger in LNHP than HNHP conditions (all $p < 0.05$) (Fig. 4N), and were 21.7–260.3% larger in HNLP than HNHP conditions (at LC: $p < 0.05$ at 80, 120 and 200 μmol photons $m^{-2} s^{-1}$, $p = 0.08$ at 320 μmol photons $m^{-2} s^{-1}$, $p > 0.1$ at 480 μmol photons $m^{-2} s^{-1}$; at HC: all $p < 0.01$ at 80–480 μmol photons $m^{-2} s^{-1}$) (Fig. 4O).

rETR values measured at 92, 133, 210, 300 and 450 μmol photons $m^{-2} s^{-1}$ of assay light intensities (A-PAR, similar to the growth light levels) were used to establish the relationships between *rETR* and photosynthetic rate or calcification rate at the growth light intensities, respectively (Fig. 5 and Table S2). Photosynthetic rates were linearly and positively correlated with *rETR* under the HNHP ($R^2 = 0.70$), LNHP ($R^2 = 0.65$) and HNLP treatments ($R^2 = 0.87$) (Fig. 5A–C). Interestingly, calcification rates were also linearly and positively related with *rETR* in HNHP ($R^2 = 0.81$), LNHP ($R^2 = 0.70$) and HNLP conditions ($R^2 = 0.83$) (Fig. 5D–F). The ratios of *rETR* to photosynthetic rate or to calcification rate were significantly affected by individually changed levels of nitrate,

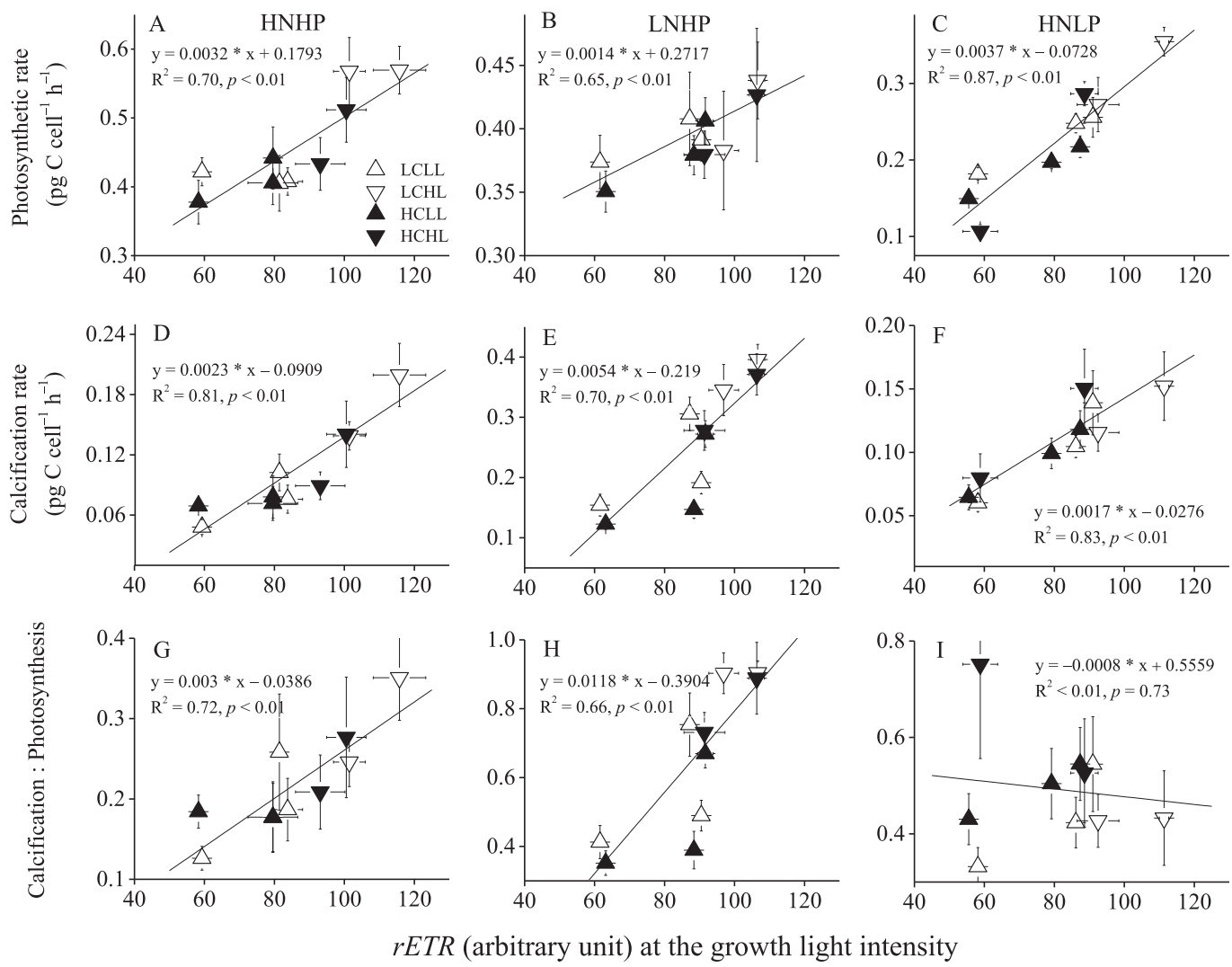

Fig. 5. Correlation of *rETR* with photosynthetic or calcification rates, or calcification to photosynthesis ratio of *E. huxleyi* cells grown under the HNHP (left), LNHP (middle) and HNLP (right) treatments, respectively. LL presents growth light intensities of 80, 120 and 200 μmol photons $m^{-2} s^{-1}$, and HL presents growth light intensities of 320 and 480 μmol photons $m^{-2} s^{-1}$. Line in each panel was fitted based on data at both LC and HC levels. *rETR* measured at 92, 133, 210, 300 and 450 μmol photons $m^{-2} s^{-1}$ of assay light levels (A-PAR) were used to establish the relationships between *rETR* and photosynthetic or calcification rates, or calcification to photosynthesis ratio at the growth light levels. The data represents the means and standard deviation of four independent experiment.

phosphate, CO_2 or light (Fig. S4 and Table S4). Our data also showed that nutrient limitation or elevated CO_2 concentration had a greater influence on photosynthetic or calcification rates than on *rETR* (Figs. 3D, E, 4A–J).

4. Discussion

In this work, we found that photosynthetic, calcification and relative electron transport rates (*rETR*) of *E. huxleyi* reached their maximal values at lower light intensities under macro-nutrient limitation and elevated level of CO_2 (Figs. 2–4), along with decreased contents of photosynthetic pigments under decreased availability of nitrate (Fig. 1). Decreased availability of phosphate, increased levels of light and CO_2 acted synergistically to reduce *ETR* (Fig. 3C and E). In addition, the relative electron transport rate positively and significantly correlated with rates of photosynthesis and calcification under the growth light levels (Fig. 5), irrespective of the nutrients availability. Our results indicate that decreased effective quantum yield (*Yield*) under nutrient limitation can be responsible for the previously observed growth reduction under high levels of CO_2 and light and nitrate or phosphate limitation [35], which supports our hypothesis.

The common photophysiological response of algae to increasing light intensities is decreasing light-harvesting pigments [30,51,52]. While lower cellular Chl *a* contents can prevent over excitation of photosystem II (PSII) and diminish reactive oxygen species (ROS) production at high light intensities [53], increased carotenoid: Chl *a* ratios under decreased availability of nutrients could allow the *E. huxleyi* cells to acclimate to high levels of light (Fig. 1L and M), since more carotenoids are expected to enhance dissipation of excessive energy and antioxidant activity [54–56]. On the other hand, in response to decreased availability of nutrients, microalgal cells usually exhibit lower metabolic activity [40,52,55,57], thus lowering demand for light in photosynthetic and calcification processes as shown here in *E. huxleyi* (Figs. 3 and 4). In addition, to acclimate to nutrient limitation and high light intensity, cells developed photoprotection strategies, such as increasing calcification rate under nitrate limitation and *NPQ* under phosphate limitation to dissipate excessive energy (Figs. 4I,J and S3F). These photoacclimation strategies decreased chlorophyll fluorescence parameters, effective photochemical quantum yield (*Yield*) and electron transport rates, though the actual electron transport may not significantly alter under nutrient limitation and high light intensity [58]. The discrepancy between the relative and actual *ETR* may be one of the reasons for lower saturating light intensity for maximal *rETR* ($rETR_{max}$) (Fig. 3A–C). Furthermore, besides the linear electron transport chain, cells grown under nutrient limitation are more likely to dissipate energy by alternative electron pathways due to lowered rates of photosynthesis and growth [59,60], including the direct photoreduction of oxygen associated with photosystem I (PSI) [61]. This may explain the observation that *rETR* reached its maximum at lower light intensity than photosynthesis under nutrient limitation (Figs. 3 and 4). Calcification has been suggested to act as an electron sink as reflected by increased non-photochemical quenching (*NPQ*) with increased calcification rate [62]. In the present work, calcification rate was positively and linearly correlated with *rETR* under different growth light levels (Fig. 5). Although the coccoliths have been suggested to play a limited role in photoprotection [63,64], our results demonstrate that calcification is an energy-dependent process [51].

Enhanced calcification rates under decreased availability of nitrate could be attributed to the extended interphase of cell division where protein synthesis and calcification occur [65,66], therefore, allowing the cells to allocate more energy to calcify, ameliorating high light-induced damage in photochemical processes [62] (Fig. 4G). In addition, decreased contents of Chl *a* with decreased availability of nitrate (Fig. 1D) might allow reallocation of nitrogen to synthesis of proteins [52,67]. On the other hand, phosphate limitation may reduce synthesis of ATP or NADPH [68], therefore, electrons from PSII facilitating the synthesis of ATP and the reduction of $NADP^+$ could be accumulated within the thylakoid lumen and in electron transport chains [53]. Consequently, reduction of the redox reaction on the reducing side of PSII can be responsible for increased *NPQ*, which dissipated more excessive energy under decreased availability of phosphate [47,52] (Fig. S3F). Nitrate or phosphate limitation in the present study decreased the photosynthetic rates, but to less extent compared to the reduction in particulate organic carbon (POC) reported in our previous work [35] (Table S3). Respiratory carbon loss during night period should be responsible for the discrepancy between POC production and photosynthetic production [69]. On the other hand, high proton concentration ($[H^+]$) induced by low pH in the culture medium under high CO_2 concentration may reduce trans-membrane H^+ electrochemical gradient and H^+ efflux rate, disturbing intracellular pH homeostasis [70], which may decrease the high light tolerance of *E. huxleyi* (Fig. 4A). Under phosphate limitation, to support cell division, *E. huxleyi* increases cellular protein synthesis and allocate less organic carbon to carbohydrate or lipid synthesis [71], so that the cells became more sensitive to high levels of light (Fig. 4E). Some studies show linear correlation between electron transport rate (*ETR*) and photosynthetic carbon fixation rate [72,73]. The positive correlation of calcification rate and *rETR* in *E. huxley*, as demonstrated in this work (Fig. 5), indicates that *rETR* can be considered as a proxy for the rates of calcification in *E. huxleyi* when grown within the light ranges of 80–200 μmol photons m^{-2} s^{-1}. In terms of ecological implications, increased calcification under nutrient limited conditions (Fig. 4I,J,N,O) may facilitate faster sinking and moves cells from nutrient limited surface waters to nutrient-richer deeper waters [74], therefore, influencing biogeochemical cycles of carbon and calcium. It is likely to use *rETR* data to predict sinking rate provided the relationship of *rETR* with calcification and sinking rates is known.

Author Contributions

Yong Zhang and Kunshan Gao designed the experiment. Yong Zhang performed this experiment. Yong Zhang and Kunshan Gao analyzed the data, wrote and improved the manuscript.

Declaration of Competing Interest

For submission of the manuscript 'Photosynthesis and calcification of the coccolithophore *Emiliania huxleyi* are more sensitive to changed levels of light and CO_2 under nutrient limitation', the authors declare that they have no conflict of interest.

Acknowledgements

This study was supported by National Natural Science Foundation of China (41806129, 41720104005, 41721005). We thank Dr. Kui Xu, Dr. Zhengke Li and Dr. Barathan Balaji for reading the manuscript and Xiangqi Yi for his help in sample taking.

Appendix A. Supplementary data

Supplementary data to this article can be found online at https://doi.org/10.1016/j.jphotobiol.2021.112145.

References

[1] K. Caldeira, M.E. Wickett, Oceanography: anthropogenic carbon and ocean pH, Nature 425 (2003) 365.
[2] M. Steinacher, F. Joos, T.L. Froelicher, L. Bopp, P. Cadule, V. Cocco, S.C. Doney, M. Gehlen, K. Lindsay, J.K. Moore, B. Schneider, J. Segschneider, Projected 21st century decrease in marine productivity: a multi-model analysis, Biogeosciences 7 (2010) 979–1005.
[3] P.W. Boyd, P.W. Dillingham, C.M. McGraw, E.A. Armstrong, C.E. Cornwall, Y. Y. Feng, C.L. Hurd, M. Gault-Ringold, M.Y. Roleda, E. Timmins-Schiffman, B. L. Nunn, Physiological responses of a Southern Ocean diatom to complex future ocean conditions, Nat. Clim. Chang. 6 (2015) 207–213.

[4] K. Gao, J. Beardall, D.P. Häder, J.M. Hall-Spencer, G. Gao, D.A. Hutchins, Effects of ocean acidification on marine photosynthetic organisms under the concurrent influences of warming, UV radiation, and deoxygenation, Front. Mar. Sci. 6 (2019) 2296–7745.
[5] L. Kwiatkowski, O. Aumont, L. Bopp, Consistent trophic amplification of marine biomass declines under climate change, Glob. Chang. Biol. 25 (2019) 218–229.
[6] B. Rost, U. Riebesell, in: H.R. Thierstein, J. Young (Eds.), Coccolithophores–From Molecular Biology to Global Impact, Springer, Berlin, 2004, pp. 99–125.
[7] L.T. Bach, U. Riebesell, M.A. Gutowska, L. Federwisch, K.G. Schulz, A unifying concept of coccolithophore sensitivity to changing carbonate chemistry embedded in an ecological framework, Prog. Oceanogr. 135 (2015) 125–138.
[8] D.M. Kottmeier, S.D. Rokitta, B. Rost, H^+-driven increase in CO_2 uptake and decrease in HCO_3^- uptake explain coccolithophores' acclimation responses to ocean acidification, Limnol. Oceanogr. 61 (2016) 2045–2057.
[9] A.J. Poulton, T.R. Adey, W.M. Balch, P.M. Holligan, Relating coccolithophore calcifcation rates to phytoplankton community dynamics: regional diferences and implications for carbon export, Deep-Sea Res. II Top. Stud. Oceanogr. 54 (2007) 538–557.
[10] P. Ziveri, B. de Bernardi, K.H. Baumann, H.M. Stoll, P.G. Mortyn, Sinking of coccolith carbonate and potential contribution to organic carbon ballasting in the deep ocean, Deep-Sea Res. II Top. Stud. Oceanogr. 54 (2007) 659–675.
[11] W. Broecker, E. Clark, Ratio of coccolith $CaCO_3$ to foraminifera $CaCO_3$ in late Holocene deep sea sediments, Paleoceanography 24 (2009), PA3205.
[12] J. Meyer, U. Riebesell, Reviews and syntheses: response of coccolithophores to ocean acidification: a meta-analysis, Biogeosciences 12 (2015) 1671–1682.
[13] U. Riebesell, P.D. Tortell, in: J.P. Gattuso, L. Hansson (Eds.), Ocean Acidification, Oxford University Press, England, 2011, pp. 99–121.
[14] I. Zondervan, B. Rost, U. Riebesell, Effect of CO_2 concentration on the PIC/POC ratio in the coccolithophore *Emiliania huxleyi* grown under light-limiting conditions and different daylengths, J. Exp. Mar. Biol. Ecol. 272 (2002) 55–70.
[15] D.M. Kottmeier, S.D. Rokitta, B. Rost, Acidification, not carbonation, is the major regulator of carbon fluxes in the coccolithophore *Emiliania huxleyi*, New Phytol. 211 (2016) 126–137.
[16] P. Jin, N. Liu, K. Gao, Physiological responses of a coccolithophore to multiple environmental drivers, Mar. Pollut. Bull. 146 (2019) 225–235.
[17] M.N. Müller, L. Beaufort, O. Bernard, M.L. Pedrotti, A. Talec, A. Sciandra, Influence of CO_2 and nitrogen limitation on the coccolith volume of *Emiliania huxleyi* (Haptophyta), Biogeosciences 9 (2012) 4155–4167.
[18] M.N. Müller, T.W. Trull, G.M. Hallegraeff, Independence of nutrient limitation and carbon dioxide impacts on the Southern Ocean coccolithophore *Emiliania huxleyi*, ISME J. 11 (2017) 1777–1787.
[19] S. Sett, L.T. Bach, K.G. Schulz, S. Koch-Klavsen, M. Lebrato, U. Riebesell, Temperature modulates coccolithophorid sensitivity of growth, photosynthesis and calcification to increasing seawater pCO_2, PLoS One 9 (2014), e88308.
[20] G. Langer, M. Geisen, K.H. Baumann, J. Klas, U. Riebesell, S. Thoms, J.R. Young, Species-specific responses of calcifying algae to changing seawater carbonate chemistry, Geochem. Geophys. Geosyst. 7 (2006), Q09006.
[21] Y. Zhang, L.T. Bach, K.T. Lohbeck, K.G. Schulz, L. Listmann, R. Klapper, U. Riebesell, Population-specific responses in physiological rates of *Emiliania huxleyi* to a broad CO_2 range, Biogeosciences 15 (2018) 3691–3701.
[22] G. Langer, G. Nehrke, I. Probert, J. Ly, P. Ziveri, Strain-specific responses of Emiliania huxleyi to changing seawater carbonate chemistry, Biogeosciences 6 (2009) 2637–2646.
[23] D. Shi, Y. Xu, F. Morel, Effects of the pH/pCO_2 control method on medium chemistry and phytoplankton growth, Biogeosciences 6 (2009) 1199–1207.
[24] K.T. Lohbeck, U. Riebesell, T.B.H. Reusch, Adaptive evolution of a key phytoplankton species to ocean acidification, Nat. Geosci. 5 (2012) 346–351.
[25] J. Beardall, J.A. Raven, in: M.A. Borowitzka, J. Beardall, J.A. Raven (Eds.), The Physiology of Microalgae, Springer, London, 2016, pp. 89–100.
[26] N.A. Gafar, K.G. Schulz, A three-dimensional niche comparison of *Emiliania huxleyi* and *Gephyrocapsa oceanica*: reconciling observations with projections, Biogeosciences 15 (2018) 3541–3560.
[27] N.A. Gafar, B.D. Eyre, K.G. Schulz, A comparison of species specific sensitivities to changing light and carbonate chemistry in calcifying marine phytoplankton, Sci. Rep. 9 (2019) 2486.
[28] B. Rost, U. Riebesell, D. Sultemeyer, D. Sültemeyer, Carbon acquisition of marine phytoplankton: effect of photoperiod length, Limnol. Oceanogr. 51 (2006) 12–20.
[29] L. Bretherton, A.J. Poulton, T. Lawson, N. Rukminasari, C. Balestreri, D. Schroeder, C. Mark Moore, D.J. Suggett, Day length as a key factor moderating the response of coccolithophore growth to elevated pCO_2, Limnol. Oceanogr. 64 (2019) 1284–1296.
[30] T. Xing, K. Gao, J. Beardall, Response of growth and photosynthesis of *Emiliania huxleyi* to visible and UV irradiances under different light regimes, Photochem. Photobiol. 91 (2015) 343–349.
[31] K. Xu, K. Gao, Solar UV irradiance modulate effects of ocean acidification on the coccolithophorid *Emiliania huxleyi*, Photochem. Photobiol. 91 (2015) 92–101.
[32] P. Jin, J. Ding, T. Xing, U. Riebesell, K. Gao, High levels of solar radiation offset impacts of ocean acidification on calcifying and non-calcifying strains of *Emiliania huxleyi*, Mar. Ecol. Prog. Ser. 568 (2017) 47–58.
[33] K. Gao, Z. Ruan, V.E. Villafañe, J.P. Gattuso, E.W. Helbling, Ocean acidification exacerbates the effect of UV radiation on the calcifiying phytoplankton *Emiliania huxleyi*, Limnol. Oceanogr. 54 (2009) 1855–1862.
[34] K. Leonardos, R.J. Geider, Elevated atmospheric carbon dioxide increases organic carbon fixation by *Emiliania huxleyi* (haptophyta), under nutrient-limited high-light conditions, J. Phycol. 41 (2005) 1196–1203.
[35] Y. Zhang, F. Fu, D.A. Hutchins, K. Gao, Combined effects of CO_2 level, light intensity and nutrient availability on the coccolithophore *Emiliania huxleyi*, Hydrobiologia 842 (2019) 127–141.
[36] Y. Zhang, S. Collins, K. Gao, Reduced growth with increased quotas of particulate organic and inorganic carbon in the coccolithophore *Emiliania huxleyi* under future ocean climate change conditions, Biogeosciences 17 (2020) 6357–6375.
[37] E. Litchman, C.A. Klausmeier, J.R. Miller, O.M. Schofield, P.G. Falkowski, Multi-nutrient, multi-group model of present and future oceanic phytoplankton communities, Biogeosciences 3 (2006) 585–606.
[38] R. Riegman, W. Stolte, A.A.M. Noordeloos, D. Slezak, Nutrient uptake and alkaline phosphatase (EC 3:1:3:1) activity of *Emiliania huxleyi* (Prymnesiophyceae) during growth under N and P limitation in continuous cultures, J. Phycol. 36 (2000) 87–96.
[39] I. Benner, U. Passow, Utilization of organic nutrients by coccolithophores, Mar. Ecol. Prog. Ser. 404 (2010) 21–29.
[40] M. Rouco, O. Branson, M. Lebrato, M.D. Iglesias-Rodríguez, The effect of nitrate and phosphate availability on *Emilinia huxleyi* (NZEH) physiology under different CO_2 scenarios, Front. Microbiol. 4 (2013) 155.
[41] C. Borchard, A. Borges, N. Händel, A. Engel, Biogeochemical response of *Emiliania huxleyi* (PML B92/11) to elevated CO_2 and temperature under phosphorus limitation: a chemostat study, J. Exp. Mar. Biol. Ecol. 410 (2011) 61–71.
[42] B. Matthiessen, S.L. Eggers, S.A. Krug, High nitrate to phosphorus regime attenuates negative effects of rising pCO_2 on total population carbon accumulation, Biogeosciences 9 (2012) 1195–1203.
[43] A. Sciandra, J. Harlay, D. Lefèvre, R. Lemée, P. Rimmelin, M. Denis, J.P. Gattuso, Response of coccolithophorid *Emiliania huxleyi* to elevated partial pressure of CO_2 under nitrogen limitation, Mar. Ecol. Prog. Ser. 26 (2003) 111–122.
[44] L. Perrin, I. Probert, G. Langer, G. Aloisi, Growth of the coccolithophore *Emiliania huxleyi* in light- and nutrient-limited batch reactors: relevance for the BIOSOPE deep ecological niche of coccolithophores, Biogeosciences 13 (2016) 5983–6001.
[45] W.G. Sunda, N.M. Price, F.M.M. Morel, in: R.A. Andersen (Ed.), Algal Culturing Techniques, Elsevier Academic Press, London, 2005, pp. 53–59.
[46] H.P. Hansen, F. Koroleff, in: K. Grasshoff, K. Kremling, M. Ehrhardt (Eds.), Methods of Seawater Analysis, WILEY-VCH Publishers, 1999, pp. 159–228.
[47] N.R. Baker, Chlorophyll fluorescence: a probe of photosynthesis in vivo, Annu. Rev. Plant Biol. 59 (2008) 89–113.
[48] P.J. Ralph, R. Gademann, Rapid light curves: a powerful tool to assess photosynthetic activity, Aquat. Bot. 82 (2005) 222–237.
[49] A.D. Jassby, T. Platt, Mathematical formulation of the relationship between photosynthesis and light for phytoplankton, Limnol. Oceanogr. 21 (1976) 540–547.
[50] H.K. Lichtenthaler, C. Buschmann, in: J. Wiley, S. Inc (Eds.), Current Protocols in Food Analytical Chemistry, Stockton Press, New York, 2001, pp. 245–252.
[51] S.D. Rokitta, B. Rost, Effects of CO_2 and their modulation by light in the life-cycle stages of the coccolithophore *Emiliania huxleyi*, Limnol. Oceanogr. 57 (2012) 607–618.
[52] Z. Li, W. Li, Y. Zhang, Y. Hu, R. Sheward, A.J. Irwin, Z.V. Finkel, Dynamic photophysiological stress response of a model diatom to ten environmental stresses, J. Phycol. (2020), https://doi.org/10.1111/jpy.13072 online.
[53] M. Ragni, R.L. Airs, N. Leonardos, R.J. Geider, Photoinhibition of PSII in *Emiliania huxleyi* (Haptophyta) under high light stress: the roles of photoacclimation, photoprotection, and photorepair, J. Phycol. 44 (2008) 670–683.
[54] K.H. Halsey, B.M. Jones, Phytoplankton strategies for photosynthetic energy allocation, Annu. Rev. Mar. Sci. 7 (2015) 265–297.
[55] S.D. Rokitta, P. von Dassow, B. Rost, U. John, P- and N-depletion trigger similar cellular responses to promote senescence in eukaryotic phytoplankton, Front. Mar. Sci. 3 (2016) 109.
[56] B.A. McKew, P. Davey, S.J. Finch, J. Hopkins, S.C. Lefebvre, M.V. Metodiev, K. Oxborough, C.A. Raines, T. Lawson, R.J. Geider, The trade-off between the light-harvesting and photoprotective functions of fucoxanthin-chlorophyll proteins dominates light acclimation in *Emiliania huxleyi* (clone CCMP 1516), New Phytol. 200 (2013) 74–85.
[57] S.D. Rokitta, P. von Dassow, B. Rost, U. John, *Emiliania huxleyi* endures N-limitation with an efficient metabolic budgeting and effective ATP synthesis, BMC Genet. 15 (2014) 1051–1064.
[58] M. Kruskopf, K.J. Flynn, Chlorophyll content and fluorescence responses cannot be used to gauge reliably phytoplankton biomass, nutrient status or growth rate, New Phytol. 169 (2006) 525–536.
[59] T. Jakob, U. Schreiber, V. Kirchesch, U. Langner, C. Wilhelm, Estimation of chlorophyll content and daily primary production of the major algal groups by means of multiwavelength-excitation PAM chlorophyll fluorometry: performance and methodological limits, Photosynth. Res. 83 (2005) 343–361.
[60] H. Wagner, T. Jakob, J. Lavaud, C. Wilhelm, Photosystem II cycle activity and alternative electron transport in the diatom *Phaeodactylum tricornutum* under dynamic light conditions and nitrogen limitation, Photosynth. Res. 128 (2016) 151–161.
[61] M.R. Badger, S. von Caemmerer, S. Ruuska, H. Nakano, Electron flow to oxygen in higher plants and algae: rates and control of direct photoreduction (Mehler reaction) and rubisco oxygenase, Philos. T. R. Soc. B. 355 (2000) 1433–1446.
[62] K. Xu, K.S. Gao, Reduced calcification decreases photoprotective capability in the coccolithophorid *Emiliania huxleyi*, Plant Cell Physiol. 53 (2012) 1267–1274.
[63] W.M. Balch, P.M. Holligan, K.A. Kilpatrick, Calcification, photosynthesis and growth of the bloom-forming coccolithophore, *Emiliania huxleyi*, Cont. Shelf Res. 12 (1992) 1353–1374.
[64] H.J. Nanninga, T. Tyrrell, Importance of light for the formation of algal blooms by *Emiliania huxleyi*, Mar. Ecol. Prog. Ser. 136 (1996) 195–203.

[65] C. Linschooten, J.D.L. van Bleijswijk, P.R. van Emburg, J.P.M. de Vrind, E. S. Kempers, P. Westbroek, E.W. de Vrind-de Jong, Role of the light-dark cycle and medium composition on the production of coccoliths by *Emiliania huxleyi* (Haptophyceae), J. Phycol. 27 (1991) 82–86.
[66] D. Vaulot, R.J. Olson, S. Merkel, S.E. Chisholm, Cell-cycle response to nutrient starvation in two phytoplankton species, *Thalassiosira weissflogii* and *Hymenomonas carterae*, Mar. Biol. 95 (1987) 625–630.
[67] K. Van Lenning, I. Probert, M. Latasa, M. Estrada, J.R. Young, in: H.R. Thierstein, J. Young (Eds.), Coccolithophores–From Molecular Biology to Global Impact, Springer, Berlin, 2004, pp. 51–73.
[68] S.T. Dyhrman, M.A. Borowitzka, J. Beardall, J.A. Raven (Eds.), The Physiology of Microalgae, Springer, Heidelberg, 2016, pp. 155–183.
[69] J.A. Raven, J. Beardall, in: J. Beardall, M.A. Borowitzka, J.A. Raven (Eds.), The Physiology of Microalgae, Springer, Heidelberg, 2016, pp. 129–140.
[70] A.R. Taylor, A. Chrachri, G. Wheeler, H. Goddard, C. Brownlee, A voltage-gated H^+ channel underlying pH homeostasis in calcifying coccolithophores, PLoS Biol. 9 (2011), e1001085, https://doi.org/10.1371/journal.pbio.1001085.
[71] B.A. McKew, G. Metodieva, C.A. Raines, M.V. Metodiev, R.J. Geider, Acclimation of *Emiliania huxleyi* (1516) to nutrient limitation involves precise modification of the proteome to scavenge alternative sources of N and P, Environ. Microbiol. 17 (2015) 1–13.
[72] P.G. Falkowski, M. Koblízek, M. Gorbunov, Z. Kolber, G.C. Papageorgiou Govindjee (Eds.), Chlorophyll *a* Fluorescence: A Signature of Photosynthesis, Springer, Netherlands, 2004, pp. 757–778.
[73] D.J. Suggett, H.L. MacIntyre, T.M. Kana, R.J. Geider, Comparing electron transport with gas exchange: parameterising exchange rates between alternative photosynthetic currencies for eukaryotic phytoplankton, Aquat. Microb. Ecol. 56 (2009) 147–162.
[74] J.A. Raven, A.M. Waite, The evolution of silicification in diatoms: inescapable sinking and sinking as escape, New Phytol. 162 (2004) 45–61.